

# Rheology of End-Tethered Polymer Layered Silicate Nanocomposites

Ramanan Krishnamoorti\*<sup>†</sup> and Emmanuel P. Giannelis\*

Department of Materials Science and Engineering, Cornell University, Ithaca, New York 14853-1501

Received April 12, 1996; Revised Manuscript Received December 27, 1996<sup>®</sup>

**ABSTRACT:** The rheology of end-tethered polymer layered silicate nanocomposites is investigated using linear viscoelastic measurements in oscillatory shear with small strain amplitudes. Two systems consisting of poly( $\epsilon$ -caprolactone) and nylon-6 with varying amounts of layered silicate (montmorillonite) are examined. The storage ( $G'$ ) and loss ( $G''$ ) moduli increase at all frequencies with increasing silicate loading, consistent with previous findings with conventionally filled polymer systems. However, the power-law dependence of  $G'$  and  $G''$  in the terminal zone is different from that observed in homopolymers and decreases with increasing silicate loading. At low frequencies the rheological response becomes almost invariant with frequency, suggestive of a solid-like response. Comparisons are drawn with rheology of other intrinsically anisotropic materials, and an attempt is made to explain phenomenologically their rich-rheological behavior.

## Introduction

Layered silicate based polymer nanocomposites are an area of active interest due to the possible technological applications as well as scientific issues concerning them.<sup>1,2</sup> Recently a better understanding of the formation and properties of these nanocomposites has been obtained using melt intercalation of polymers into layered silicates above the softening temperature of the polymer.<sup>3</sup> Depending on the interaction between the layered silicate (which is typically organically modified by replacing the charge-balancing interlayer cations with alkyl ammonium ions in order to render the silicate layers organophilic) and the polymeric species, different microstructured nanocomposites ranging from immiscible to intercalated to delaminated are possible. In intercalated nanocomposites, a single, extended polymer chain is inserted between the silicate layers, resulting in a well-ordered multilayer with a repeat distance of a few nanometers, while in delaminated hybrids the silicate layers (1 nm thick) are exfoliated and dispersed in a continuous polymer matrix.

From processing and application points of view, the mechanical and rheological properties of these nanocomposites are of vital importance. It would also be important to relate their mechanical and rheological properties to the nature and microstructure of the nanocomposites formed. Furthermore these nanocomposites appear to be an ideal system to probe the dynamics and statics of confined polymers.<sup>4</sup>

An important class of polymer layered silicate nanocomposites is prepared by *in situ* polymerization of certain monomers with the initiating species tethered to the silicate surface (Figure 1).<sup>5–8</sup> These nanocomposites show dramatic improvements in permeability, mechanical, and thermal properties.<sup>6,8</sup> This paper focuses on understanding the rheological properties of end-tethered polymer layered silicate nanocomposites. Two series of delaminated hybrids based on poly( $\epsilon$ -caprolactone) (PCL) and nylon-6 are examined. The silicate layers used in these samples are highly anisotropic with aspect ratios of  $\sim 100$ – $1000$ , with lateral

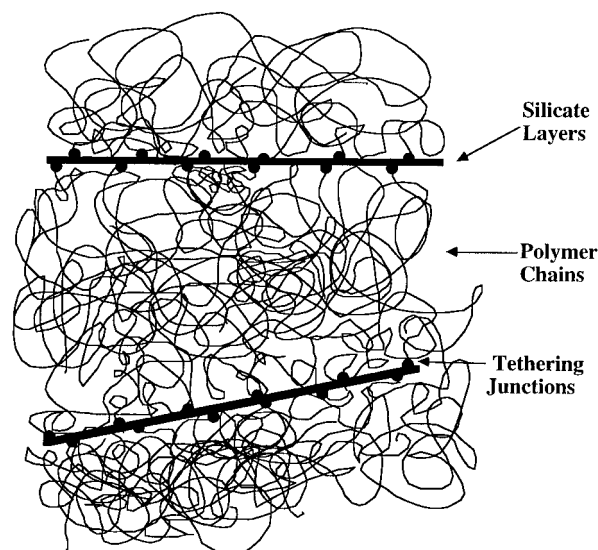


**Figure 1.** Schematic diagram describing the end-tethered nanocomposites. The layered silicates are highly anisotropic with a thickness of 1 nm and lateral dimensions (length and width) ranging from several 100 nm to a few microns. The polymer chains are tethered to the surface via ionic interactions between the silicate layer and the polymer end.

dimensions of 100–1000 nm. Considering the surface charge density of the montmorillonite (with charge exchange capacities (in mequiv/100 g) of 100 in the PCL series and 120 in the nylon-6 series), the surface area occupied per chain is calculated to be 0.59 and 0.48 nm<sup>2</sup>, respectively. It is well-known that naturally occurring layered silicates (such as montmorillonite) are inhomogeneous across layers, and hence such a surface area calculation serves only as an approximate guide. Such a high-average grafting density (with the areal density of grafting  $\times$  unperturbed radius of gyration  $\gg 1$ ) causes these systems to be excellent model systems to understand the static conformations and dynamics of polymer brushes. These are of intense theoretical, experimental, and simulation interest due to the variety of practical problems that can be modeled on the basis of the ideas garnered on polymer brushes,<sup>9</sup> and the study of these systems as model polymer brushes will be the subject of a separate publication.<sup>10</sup> In this paper we focus on the linear viscoelastic behavior of these end-tethered

<sup>†</sup> Current address: Department of Chemical Engineering, University of Houston, Houston, TX 77204.

<sup>®</sup> Abstract published in *Advance ACS Abstracts*, June 15, 1997.

**Table 1. Molecular Weights of Recovered Poly( $\epsilon$ -caprolactone)<sup>a,d</sup>**

sample <sup>b</sup>	wt % OMTS	vol % MTS <sup>c</sup>	$\bar{M}_w$	$\bar{M}_n$	$\bar{M}_w/\bar{M}_n$
PCLC1	1	0.4	30 900	17 200	1.8 <sub>0</sub>
PCLC2	2	0.8	16 900	10 300	1.6 <sub>4</sub>
PCLC3	3	1.2	14 500	9 200	1.5 <sub>7</sub>
PCLC5	5	2.0	13 600	8 800	1.5 <sub>4</sub>
PCLC10	10	4.0	16 000	9 900	1.6 <sub>3</sub>

<sup>a</sup> GPC performed on polymer recovered from PCLC samples using ion exchange reaction. <sup>b</sup> Number at end of acronym indicates wt % OMTS in the composite. <sup>c</sup> Calculated assuming full conversion of CL to PCL, using specific densities of 1.2 g/cc (PCL) and 2.5 g/cc (MTS) to convert from wt % OMTS to vol. % MTS. <sup>d</sup> MTS = Mica-type silicate; OMTS = organically modified mica-type silicate; CL =  $\epsilon$ -caprolactone; PCL = poly( $\epsilon$ -caprolactone).

**Table 2. Characterization of Nylon-6 Montmorillonite Hybrids**

sample	wt % MTS	$\bar{M}_w$
nylon-6	0	21 700
nylon-6-2	2	22 200
nylon-6-5	5	19 700

nanocomposites and examine them as model systems to understand intrinsically anisotropic layered materials.

## Experimental Section

The preparation of the end-tethered poly( $\epsilon$ -caprolactone)–montmorillonite nanocomposites have been described in a previous publication.<sup>8</sup> The end-tethered composites were prepared by first converting the silicate surface from a hydrophilic to an organophilic surface by an ion exchange of the metal cations by 12-aminolauric acid. The polymerization of  $\epsilon$ -caprolactone is then initiated by the carboxyl groups of the aminolauric acid and the polymerization proceeds via a ring opening of the  $\epsilon$ -caprolactone. The polymer is bound to the silicate layers through the protonated amine terminus. Characterization of the nanocomposites and the polymer (recovered by a reverse ion exchange reaction) by X-ray diffraction (XRD), differential scanning calorimetry, IR, and gel permeation chromatography (GPC) measurements have also been reported earlier.<sup>8</sup> XRD studies show the absence of any stacking of the silicate, suggesting that the host layers are well dispersed in the polymer matrix. The molecular weight characterization is reproduced in Table 1. The PCL molecular weight shows a monotonic decrease when the silicate content increases from 1 to 5%, with the 10% silicate sample being an anomaly possibly due to the formation of a gel upon incorporation of the monomer as well as due to well-known hydrogen transfer reactions during the polymerization step. Rheology samples were prepared by first dissolving the polymers in toluene and then allowing the samples to dry for a week above the melting temperature of poly( $\epsilon$ -caprolactone), so as to erase any effects of alignment of the layered compounds during their formation. Samples were allowed to flow and form a 25 mm diameter disc with a thickness of roughly 2 mm.

Another system studied was a series of end-tethered nylon-6 silicate nanocomposites prepared by Ube Industries Ltd. and kindly provided by them. Three samples—a pure nylon-6, a 2 wt % sample, and a 5 wt % sample, whose descriptions (as provided by Ube Industries Ltd.) are provided in Table 2—were examined at a single temperature of 235 °C under an argon atmosphere. Rheological samples were prepared by compression molding with small compressive stresses (identical in all cases and only to the extent provided by placing an aluminum plate of dimensions 2" × 2" × 0.1" on top) of the as-received pellets at 235 °C.

Rheology measurements were performed on a Rheometrics RDA-II, in oscillatory mode with a parallel plate geometry using 25 mm diameter plates. All measurements were performed with a 200 g cm transducer with a lower resolution limit of 0.2 g cm over as wide a frequency range as possible.

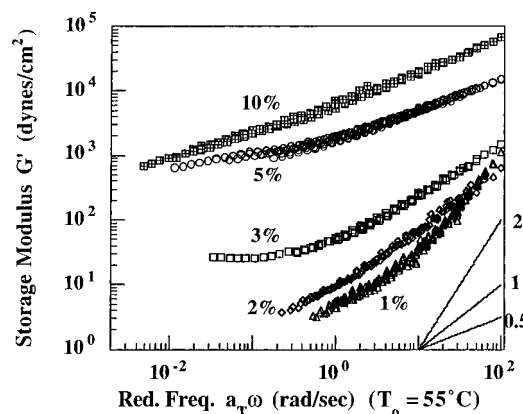


**Figure 2.** Storage modulus ( $G'$ ) for PCL-based silicate nanocomposites. Silicate loadings are indicated in the figure. Master-curves were obtained by application of time–temperature superposition and shifted to  $T_0 = 55$  °C. (See text and Figure 4.)

Typical sample thickness ranged from 1.6 to 1.8 mm. Some measurements were also performed with thinner samples (thickness  $\approx 0.8$ –1.2 mm), to ensure negligible surface effects were present due to possible surface-induced ordering of the layered structure. The data for the thinner samples were in good agreement with those from the thicker samples (with an error of  $\pm 1\%$ ), indicative of little or no influence of the surface on the microstructure. Rheological measurements on the PCL-based nanocomposites were conducted over a temperature range of 55–160 °C. The rheological properties were reproducible after repeated temperature cycling, indicating no additional alignment induced, chain degradation during measurements, or condensation effects that might affect the stability of the melt. All the data presented in this paper have been verified to be in the linear regime by probing at higher (and in some cases also lower) strain amplitudes and have been found to be independent of strain amplitude.

Some rheological measurements were also performed with large-amplitude oscillatory shear, in order to induce global alignment of the silicate layers. The shear stress was recorded as a function of time and was found to vary in a sinusoidal manner (the higher harmonics, i.e., 3 and 5 $\omega$  were much smaller than the primary harmonic) throughout the experiments, thereby facilitating the determination of the during-shear storage and loss moduli. Small strain (linear viscoelastic) measurements were performed before and after these large-amplitude oscillatory shear experiments, so as to quantify the effect of alignment. While some preliminary results of these measurements are presented in this paper, we are currently using SANS and SAXS to investigate the induced order as well as studying the linear and nonlinear rheological properties of these materials.

## Results and Discussion

The linear viscoelastic response as measured by the storage and loss moduli ( $G'$  and  $G''$ , respectively) for the five PCL nanocomposites examined is shown in Figures 2 and 3, respectively. Data were acquired at several temperatures using the lowest possible strain amplitudes (typically in the range of 0.1–5.0%) and shifted using the time–temperature superposition principle to form the master curves presented in Figures 2 and 3. For the low silicate content nanocomposites (1, 2, and 3 wt %) only a horizontal (frequency) shift ( $a_T$ ) was incorporated as there were no features present in the moduli data to warrant a vertical (modulus) shift. For the higher silicate content nanocomposites (5 and 10 wt %), a small temperature dependent vertical (modulus) shift factor ( $b_T$ ;  $0.9 < b_T < 1.0$ ) was incorporated along with the frequency shift factor to ascertain good superposition in the low-frequency regime. The frequency

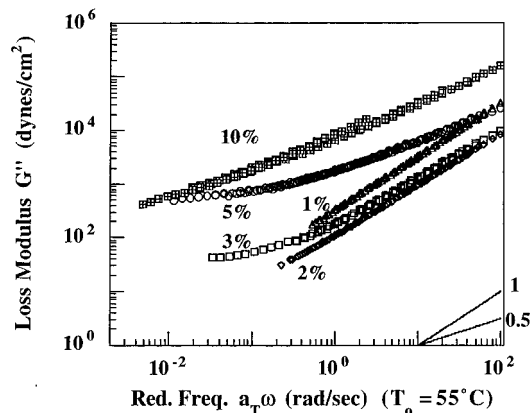


**Figure 3.** Loss modulus ( $G''$ ) for PCL-based silicate nanocomposites. Same as Figure 2.

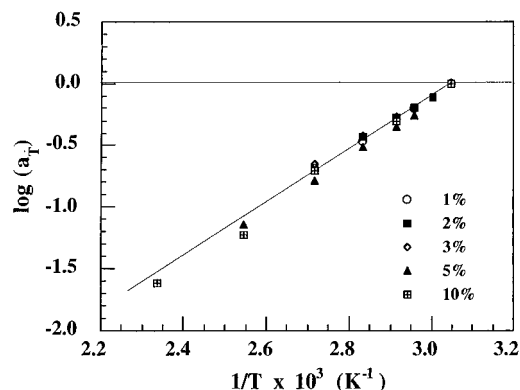


**Figure 4.** Frequency shift factors ( $a_T$ ) as a function of temperature for PCL-based nanocomposites. Solid line corresponds to shift factors for pure poly( $\epsilon$ -caprolactone).

shift factors for all the samples as a function of temperature are shown in Figure 4. The linearity of the measurement was verified by reproducing the data using higher strain amplitudes as well as by recording the signal on a strip chart recorder and ensuring that the output force signal was sinusoidal with the higher harmonics being significantly smaller than the primary signal. Furthermore, for all the composites examined, the data was somewhat restricted due to the alignment of the silicate layers by the application of large amplitude oscillatory shear (particularly required at low frequencies, to obtain force signals larger than the low limit of the transducer). This was particularly restrictive for the high silicate loading composites (PCLC5 and PCLC10) wherein at high temperatures and low frequencies alignment of the layers would start to occur (as measured by a change in the rheological response consistent with alignment of the layers) at strain amplitudes as low as 10%. Only data verified to be in the linear regime are shown in Figures 2 and 3.

The storage moduli (Figure 2) for the nanocomposites show a monotonic increase at all frequencies with increasing silicate content, with the exception of PCLC2, where at the highest frequencies, it has a slightly lower value than PCLC1. The loss moduli (Figure 3), on the other hand, show a somewhat nonmonotonic dependence, with the value for PCLC1 exceeding that for PCLC2, PCLC3, and PCLC5. However, the trend for the 2–10 wt % samples suggests that  $G''$  increases with increasing silicate loading. In this context, it is worthwhile to note the trend of decreasing molecular weight of the poly( $\epsilon$ -caprolactone) with increased silicate loading (Table 1). The largest decrease occurs from 1 to 2

**Table 3.** High-Frequency Slope of  $G'$  and  $G''$  vs  $\omega$  for PCLC

sample	$G'$	$G''$
PCLC1	1.6 <sub>0</sub>	1.0 <sub>0</sub>
PCLC2	0.9 <sub>7</sub>	0.9 <sub>7</sub>
PCLC3	0.8 <sub>0</sub>	0.9 <sub>0</sub>
PCLC5	0.5 <sub>0</sub>	0.6 <sub>5</sub>
PCLC10	0.5 <sub>5</sub>	0.7 <sub>0</sub>

wt % silicate loading, while the molecular weight of the polymer chains in the 2, 3, 5, and 10% nanocomposites is nearly the same.

For the molecular weights of the PCL samples examined here, it is expected that, at the temperatures and frequencies at which the rheological measurements were carried out, the polymer chains should be fully relaxed and exhibit characteristic homopolymer-like terminal behavior, i.e.,  $G' \propto \omega^2$  and  $G'' \propto \omega$  (based on the relaxation behavior of pure PCL, the data presented in Figures 2 and 3 are those corresponding to frequencies below the cross-over frequency associated with the transition from the plateau to the terminal relaxation of the polymer). While the polydispersity of the polymer chain lengths would affect this behavior, the effect is expected to be small in the dynamic regimes probed. The high-frequency-regime frequency dependence of the storage modulus decreases monotonically with increased silicate loading from  $\omega^{1.65}$  for PCLC1 to  $\omega^{0.5}$  for PCLC5. The frequency dependence of  $G''$  also progresses monotonically with silicate loading, depending as  $\omega^{1.0}$  for PCLC1 to  $\omega^{0.65}$  for PCLC5. The high-frequency power-law dependence of  $G'$  and  $G''$  for all the samples is summarized in Table 3.

Interestingly, the frequency shift factors for the PCLC samples appear to be independent of the silicate loading, consistent with the results for the frequency shift factors previously obtained for PCL (Figure 4).<sup>11</sup> Due to the low  $T_g$  of PCL ( $\sim -60$  °C) and the measurements being performed at temperatures greater than 55 °C (due to the crystallization of PCL), the temperature-dependent frequency shift factors are relatively small. The flow activation energy obtained by fitting the data at all silicate loadings is estimated to be 19 kJ/mol. Measurements on a PCL homopolymer (Aldrich Chemicals with  $M_w = 90$  k) over the same temperature range yielded a value of 17 kJ/mol, in good agreement with the results for the PCL nanocomposites. This agreement implies that the temperature dependence of the relaxation being probed is that of the polymer. Since the silicate layers to which the polymers are tethered do not have a temperature dependent relaxation, the only relaxation process probed as a function of temperature is that of the polymer segments. It is thus reasonable to expect that these nanocomposites would exhibit time–temperature superposition as well as exhibit temperature shift factors similar to that of the homopolymer.

Similar rheological behavior was also observed with the nylon-6 silicate hybrids. Figures 5 and 6 show the storage and loss moduli recorded at 235 °C for the three samples.<sup>4</sup> Both  $G'$  and  $G''$  exhibit a monotonic increase with increasing silicate loading at all frequencies. Unlike the PCL nanocomposites, the molecular weight of the polymer matrix is nearly the same for all three nylon samples (Table 2). This result further suggests that the inconsistency observed in the PCL nanocomposites with the 1 wt % sample showing a higher  $G'$  value than that for the 2 wt % sample may be caused by the abrupt decrease in molecular weight in the latter sample.

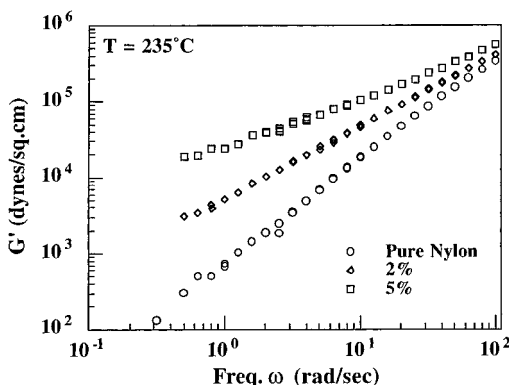


**Figure 5.** Storage modulus ( $G'$ ) for nylon-6 silicate hybrids. Silicate loadings are indicated in the figure. All measurements were carried out at a single temperature of 235 °C.

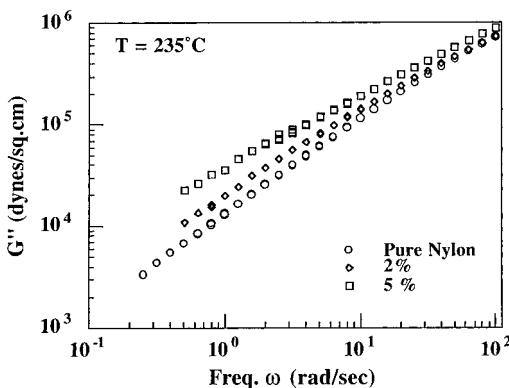


**Figure 6.** Loss modulus ( $G''$ ) for nylon-6 silicate hybrids. Same as Figure 5.

**Table 4. Terminal Slopes of  $G'$  and  $G''$  vs  $\omega$  for Nylon-6 Silicate Hybrids**

sample	$G'$	$G''$
nylon-6	1.5 <sub>0</sub>	0.9 <sub>3</sub>
nylon-6-2	1.0 <sub>0</sub>	0.8 <sub>0</sub>
nylon-6-5	0.6 <sub>0</sub>	0.7 <sub>0</sub>

Terminal zone slopes were estimated for all three samples at frequencies below 10 rad/s and are reported in Table 4. In close analogy to the PCL-based nanocomposites, the terminal zone dependence of  $G'$  and  $G''$  for the 2 and 5 wt % samples show nonterminal behavior with power-law dependencies for  $G'$  and  $G''$  much smaller than the expected 2 and 1, respectively. Furthermore, like the PCL-based nanocomposites, there also appears to be a gradual decrease in the power-law dependence of  $G'$  and  $G''$  with increasing silicate loading. However, because data could only be obtained at a single temperature of 235 °C, we are unable to compare the temperature dependence of the relaxation observed in these nanocomposites (as inferred from the temperature shift factors) to those of the homopolymer.

Figures 2–6 illustrate several aspects unique to the rheological properties of these nanocomposites. Time-temperature superposition can be applied to the low-amplitude oscillatory shear rheological response, with temperature shift factors being similar to that of the pure polymer. Holding the molecular weight relatively constant (the nylon-6 series and PCLC2–PCLC10) reveals that at any given frequency the magnitude of the storage and loss moduli increase monotonically with increasing silicate loading. Furthermore, the frequency dependence of the high-frequency behavior of  $G'$  and  $G''$  shows a gradual change with increasing silicate loading—from homopolymer-like behavior at low silicate

loading to increasingly nonterminal behavior at higher silicate contents—and finally plateauing at  $G'$  and  $G'' \propto \omega^{0.5}$  for silicate loadings of greater than 5 wt %. Finally, at the very lowest shear rates accessed, these nanocomposites exhibit a low-frequency behavior that has both  $G'$  and  $G''$  almost independent of frequency. We discuss these aspects of the rheological response in the following parts of this paper.

The frequency dependence of the storage and loss moduli of these end-tethered nanocomposites can be contrasted to those observed in a series of delaminated hybrids with no end-tethering.<sup>4</sup> In the latter, a monotonic increase in the moduli at all frequencies was observed with no observable change in the frequency dependence from that of the polymer for hybrids containing as much as 20 wt % layered silicate. Nonterminal flow behavior has been observed in filled-polymer systems exhibiting yield phenomena, but only in cases wherein the filler and polymer are actively interacting and in a dynamic regime controlled by much larger length scales (i.e., lower frequencies) than those observed in this study. Furthermore, the deviations from homopolymer-like behavior in these systems have been observed at relatively high filler loadings. At similar high silicate loadings in either exfoliated or intercalated hybrids (not tethered to the silicate surface), we have observed significant nonlinear rheological behavior, thereby complicating the data analysis.<sup>12</sup> The analogies with filled polymer systems may have particular relevance to the low-frequency behavior of the storage modulus in the PCLC nanocomposites and are discussed in greater detail below.

Nonterminal low-frequency rheological behavior has also been observed in ordered block copolymers and smectic liquid-crystalline small molecules.<sup>14,15</sup> Several hypotheses have been suggested to explain the observed rheological behavior in these systems.<sup>14–20</sup> Koppi et al. have suggested that undulations and defects in the layers might contribute to the low-frequency viscoelastic response in layered block copolymers.<sup>14</sup> Other ideas include that the domain structure of the ordered mesophases is responsible, due to the dynamic processes on both the microscopic and mesoscopic length scales. It is also well documented that topological defects also affect rheological properties dramatically, particularly in the low-frequency terminal regime.<sup>15</sup> Effects of domain collective dynamics were studied by Kawasaki and Onuki,<sup>16</sup> who demonstrated that overdamped second-sound modes in an orientationally disordered lamellar phase could result in anomalous low-frequency rheological behavior. Rubinstein and Obukhov<sup>17</sup> also obtained the same result by considering diffusion-controlled annihilation of defects in a disordered lamellar system. The results of Larson et al.<sup>15</sup> with smectic small molecules and short ordered block copolymers has suggested that the nonterminal low-frequency response is due to the long-range domain structure and the presence of defects.

The silicate layers in the hybrids are highly anisotropic with lateral dimensions ranging 100–1000 nm, and even when separated by large distances (i.e., when delaminated) cannot be placed completely randomly in the sea of polymer. Furthermore, the majority of the polymer chains in the hybrids are tethered to the surface of the silicate layers. Thus, it can be expected that there are domains in these materials, even above the melting temperature of the constituent polymers, wherein some long-range order is preserved and the

silicate layers are oriented in some preferred direction. Furthermore, this long-range order and domain structure is likely to become better defined at the higher silicate contents, where the geometrically imposed mean distance between the layers becomes less than the lateral dimensions of the silicate layers and thus forcing some preferential orientation between the layers. However, there is likely to be considerable polydispersity effects in terms of the orientation and the distance between the silicate layers. Many such randomly oriented grains make up the entire sample leading to the presence of a disordered material. Thus, in general, the material possesses a layered structure, with grains wherein the silicate layers are oriented in a preferred direction leading to the presence of grain boundaries and the concomitant presence of defects. However, on the basis of our results on delaminated hybrids with no end tethering, wherein we observe an increase in the moduli at all frequencies and classical homopolymer-like terminal behavior, it appears that delamination alone is not sufficient to produce the nonterminal flow behavior.

The nonterminal low-frequency behavior observed in the PCL- and nylon-6-based nanocomposites could also be attributed to the retardation of molecular relaxation processes produced by the tethering of one end of these molecules to the silicate surface. Witten et al.<sup>20</sup> have suggested that tethering of the polymer molecules is expected to create an energetic barrier to the reptation motion, which leads to a dramatic increase in the relaxation time and hence a shift of the terminal relaxation to very low frequencies. Since the molecular weight of the samples examined here is small, it is expected that the dominant relaxation mode would be Rouse-like, which should not be drastically slowed by the tethering of one end of the chains. Furthermore, at all silicate loadings, most of the chains are tethered to the silicate layers, and any effect of the tethering should be discernible at all loadings.<sup>21</sup> However, from the data presented in this paper (see Tables 3 and 4), it is clear that the terminal-zone behavior gradually changes with increased silicate loading, saturating at about 5 wt %.

Of particular interest in Figures 2 and 3 is the presence of a transition from the slopes observed at high frequency to a more flattened behavior at low frequencies. The change is more pronounced in the case of  $G'$  than  $G''$ . The low-frequency response is indicative of a "pseudo-solid-like" behavior and is clearly seen in the PCL samples with silicate loading greater than 3 wt %. A similar rheological response at low frequencies has been observed in triblock copolymers in the ordered state and has been attributed to the quasi-tethering of the unlike polymer segments in their respective microdomains.<sup>22</sup> Solid-like response has also been observed in conventionally filled polymer systems in which there were strong interactions between the polymer and the filler and has been attributed to the presence of yield phenomena in these systems.<sup>23</sup> Thus, the presence of the silicate layers and the lack of complete relaxation of the chains contribute to the pseudo-solid-like response at low frequencies (pseudo-solid-like because  $G'$  does not exceed  $G''$  by orders of magnitude as would be expected from a true solid).

Application of large-strain-amplitude oscillatory shear leads to a shear-aligned sample. These measurements were carried out on the 3, 5, and 10% samples, and the during-shear moduli show a decrease with continual

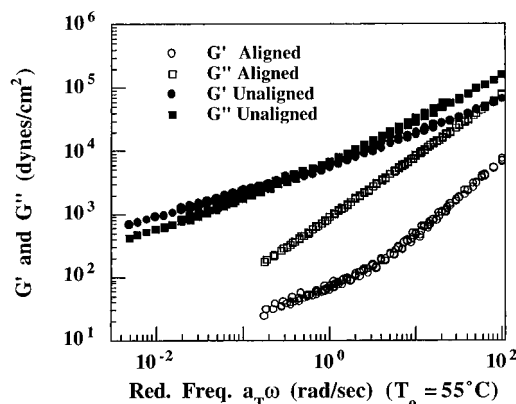


**Figure 7.**  $G'$  and  $G''$  obtained using small-amplitude oscillatory strain for PCLC10 before and after large-amplitude shear. See text for conditions of large-amplitude shear.

shearing and finally reach a plateau value. With the exception of the first few cycles of shear for the 3 and 5% samples, the modulus decreases monotonically and the stress signal remains sinusoidal. In the first few cycles of shear for the 3 and 5% samples, the moduli show a maximum, before monotonically decreasing. The small-strain moduli after shear alignment for PCLC10 carried out at  $T = 70\text{ }^{\circ}\text{C}$ ,  $\omega = 1\text{ rad/s}$ ,  $\gamma_0 = 120\%$ , and time = 3 h are shown in Figure 7. First, both the storage and loss moduli for the aligned sample are considerably lower than that for the initially unaligned sample. Secondly, the frequency dependence of both  $G'$  and  $G''$  for the aligned samples are much stronger and start to resemble those of free homopolymers. The small-strain modulus results observed for the PCLC samples before and after shear alignment are in close analogy with those observed for block copolymers as well as small molecule smectic liquid crystals.<sup>15,24</sup> The temperature-dependent frequency-shift factors for the aligned and initially unaligned sample are identical within experimental error. That large-amplitude oscillatory shear can significantly alter the (small-strain) linear viscoelastic response indicates that there is some mesoscopic arrangement of the silicate layers, which is organized by the application of large-amplitude shear. We are currently examining the shear-aligned materials using SANS, SAXS, and rheological measurements in order to fully characterize and understand the dynamic processes associated with these materials.<sup>10</sup> In fact, preliminary SANS measurements on post large-amplitude oscillatory shear confirm the presence of global alignment of the silicate layers.

In the light that the application of prolonged large-amplitude shear can affect the linear viscoelastic properties of these nanocomposites, it is worthwhile to reexamine the slightly increased power-law dependence of the terminal regime in the nylon-6-based nanocomposites as compared to that of the PCL-based nanocomposites at comparable silicate loading (Tables 3 and 4). The nylon-6 samples were obtained as extruded pellets, thereby subjected to some shear or elongation history and were formed into disks for rheology by compression molding at  $235\text{ }^{\circ}\text{C}$ . This sample treatment (particularly the formation of pellets) might have led to a small amount of alignment of the layered silicates, at least near the surface of each pellet. In fact, work by Kojima et al.<sup>25</sup> on nylon-6/silicate hybrids have shown that, for samples prepared by injection molding, the region near the surface shows significant orientation along the flow direction, while in the center of the samples the silicate

layers are randomly oriented. While rheological measurements carried out with samples with different thicknesses within experimental error yielded identical results, the alignment caused by extrusion might have resulted in the slightly increased power-law dependence in the nylon nanocomposites.

### Concluding Remarks

The end-tethered polymer layered silicate nanocomposites have been shown to exhibit a rich variety of rheological properties. In addition, understanding the rheological behavior of nanocomposites could elucidate the dynamics of intrinsically anisotropic materials such as block copolymers and liquid crystalline polymers. Similarities of the rheological response of end-tethered nanocomposites on one hand and block copolymers and smectic liquid crystals on the other have been demonstrated.

Several important points need to be noted. First, the mere presence of anisotropic layered material without an active interaction between the soft and hard phase does not lead to the nonterminal rheological behavior.<sup>4</sup> Second, the power-law dependence of the terminal region shows a dependence on the concentration of the layered silicates and saturates at ~5 wt % of silicates. Thirdly, the systems examined in this study which show nonterminal rheological behavior have molecular weights which would only be marginally entangled, reiterating claims made with lamellar block copolymers and smectic liquid crystals that the presence of entanglements is not required to observe the nonterminal behavior.

**Acknowledgment.** This work was supported by generous gifts from DuPont, Exxon, Hoechst Celanese, Hercules, Monsanto, Nanacor, Southern Clay Products, and Xerox. We acknowledge Phil Messersmith for synthesizing the PCL samples as well-valuable discussions. Ube Industries Ltd., is also acknowledged for providing the nylon samples. We would like to thank C. Cohen for kindly allowing us to use the rheometer. Valuable discussions with E. J. Kramer, E. Manias, and S. D. Burnside are also gratefully acknowledged.

### References and Notes

- (1) Brus, L. E.; Brown, W. L.; Andres, R. P.; Averback, R. S.; Goddard, W. A., III; Kaldor, A.; Louie, S. G.; Moskovits, M.; Percy, P. S.; Riley, S. J.; Siegel, R. W.; Spaepen, F. A.; Wang, Y. *J. Mater. Res.* **1989**, *4*, 704; National Research Council. *Research Opportunities for Materials with Ultrafine Microstructures*; National Academy Press: Washington, DC, 1989.
- (2) Giannelis, E. P.; Mehrotra, V.; Tse, O. K.; Vaia, R. A.; Sung, T.-C. *Synthesis and Processing of Ceramics: Scientific Issues*; Rhine, W.E., Shaw, M. T., Gottshall, R. J., Chen, Y. Eds.; *MRS Proceedings* **1992**, *249*, 547; Yano, K.; Usuki, A.; Kurauchi, T.; Kamigaito, O. *J. Polym. Sci., Part A: Polym. Chem.* **1993**, *31*, 2493.
- (3) Vaia, R. A.; Ishii, H.; Giannelis, E. P. *Chem. Mater.* **1993**, *5*, 1694; Vaia, R. A.; Teukolsky, R. K.; Giannelis, E. P. *Chem. Mater.* **1994**, *6*, 1017; Vaia, R. A.; Vasudevan, S.; Krawiec, W.; Scanlon, L. G.; Giannelis, E. P. *Adv. Mater.* **1995**, *7*, 154; Vaia, R. A.; Giannelis, E. P. Submitted to *Macromolecules*; Vaia, R. A.; Jandt, K. D.; Kramer, E. J.; Giannelis, E. P. *Macromolecules* **1995**, *28*, 8180; Vaia, R. A.; Giannelis, E. P. Submitted to *Macromolecules*, **1995**; Vaia, R. A. Ph.D Thesis, Cornell University, 1995.
- (4) Krishnamoorti, R.; Vaia, R. A.; Giannelis, E. P. *Chem. Mater.* **1996**, *8*, 1728.
- (5) Kojima, Y.; Usuki, A.; Kawasumi, M.; Okada, A.; Kurauchi, T.; Kamigaito, O. *J. Polym. Sci., Part A: Polym. Chem.* **1993**, *31*, 983.
- (6) Usuki, A.; Kawasumi, M.; Kojima, Y.; Okada, A.; Kurauchi, T.; Kamigaito, O. *J. Mater. Res.* **1993**, *8*, 1174; Usuki, A.; Kojima, Y.; Kawasumi, M.; Okada, A.; Fukushima, Y.; Kurauchi, T.; Kamigaito, O. *J. Mat. Res.* **1993**, *8*, 1179.
- (7) Messersmith, P. B.; Giannelis, E. P. *Chem. Mater.* **1993**, *5*, 1064.
- (8) Messersmith, P. B.; Giannelis, E. P. *J. Polym. Sci., Part A: Polym. Chem.* **1995**, *33*, 1047.
- (9) Lai, P.-Y. *Flow-Induced Structure in Polymers*; Nakatani, A. I., Dadmun, M. D., Eds.; ACS Symposium Series; American Chemical Society: Washington, DC, 1995; Vol. 597, p 204; Joanny, J.-F. *Langmuir* **1992**, *8*, 989; Semenov, A. N. *Langmuir* **1995**, *11*, 3560; Milner, S. T. *Science* **1991**, *251*, 905.
- (10) Krishnamoorti, R.; Giannelis, E. P. Manuscript in preparation.
- (11) Jo, W. H.; Chae, S. H.; Lee, M. S. *Polym. Bull.* **1992**, *29*, 113; Han, C. D.; Yang, H.-H. *J. Appl. Polym. Sci.* **1987**, *33*, 1199.
- (12) Krishnamoorti, R.; Giannelis, E. P. Unpublished data.
- (13) The somewhat lower than expected frequency dependence of  $G'$  and  $G''$  for the pure nylon-6 might be caused by the proximity to the crossover frequency, polydispersity effects, and long-chain branching caused during the polymerization or subsequent processing at elevated temperatures.
- (14) Rosedale, J. H.; Bates, F. S. *Macromolecules* **1990**, *23*, 2329; Koppi, K. A.; Tirrell, M.; Bates, F. S.; Almdal, K.; Colby, R. H. *J. Phys. II (Paris)* **1993**, *2*, 1941.
- (15) Larson, R. G.; Winey, K. I.; Patel, S. S.; Watanabe, H.; Bruinsma, R. *Rheol. Acta* **1993**, *32*, 245.
- (16) Kawasaki, K.; Onuki, A. *Phys. Rev. A* **1990**, *42*, 3664.
- (17) Rubinstein, M.; Obukhov, S. P. *Macromolecules* **1993**, *26*, 1740.
- (18) Halperin, A.; Tirrell, M.; Lodge, T. P. *Adv. Polym. Sci.* **1992**, *100*, 31.
- (19) Ohta, T.; Enomoto, Y.; Harden, J. L.; Doi, M. *Macromolecules* **1993**, *26*, 4928; Doi, M.; Harden, J. L.; Ohta, T. *Macromolecules* **1993**, *26*, 4935.
- (20) Witten, T. A.; Leibler, L.; Pincus, P. *Macromolecules* **1990**, *23*, 824.
- (21) Recently we have conducted rheological experiments wherein the end-tethered PCL nanocomposites were blended with a pure PCL homopolymer. Rheological behavior, particularly the terminal zone slopes, obtained for 5 wt % and 10 wt % (obtained by blending equal weight fractions of the PCL homopolymer with a 10 wt % PCL and 20 wt % PCL, respectively) were found to be similar to those obtained from the as-prepared nanocomposites.
- (22) Watanabe, H.; Kuwahara, S.; Kotaka, T. *J. Rheol.* **1984**, *28*, 393; Adams, J. L.; Graessley, W. W.; Register, R. A. *Macromolecules* **1994**, *27*, 6026.
- (23) Agarwal, S.; Salovey, R. *Polym. Engg. and Sci.* **1995**, *35*, 1241.
- (24) Patel, S. S.; Larson, R. G.; Winey, K. I.; Watanabe, H. *Macromolecules* **1995**, *28*, 4313.
- (25) Kojima, Y.; Usuki, A.; Kawasumi, M.; Okada, A.; Kurauchi, T.; Kamigaito, O.; Kaji, K. *J. Polym. Sci.: Part B: Polym. Phys.* **1994**, *32*, 625; Kojima, Y.; Usuki, A.; Kawasumi, M.; Okada, A.; Kurauchi, T.; Kamigaito, O.; Kaji, K. *J. Polym. Sci., Part B: Polym. Phys.* **1995**, *33*, 1039.

MA960550A